Nonlinear Feedback Control and Artificial Intelligence Computational Methods applied to a Dissipative Dynamic Contact Problem

Daniela Danciu[1], Andaluzia Cristina Matei [2], Sorin Micu [2,3] and Ionel Roventa[2]
[1]*Department of Automation, Electronics and Mechatronics, University of Craiova, 200585, Craiova, Romania*
[2]*Department of Mathematics, University of Craiova, 200585, Craiova, Romania*
[3]*Institute of Mathematical Statistics and Applied Mathematics, 70700, Bucharest, Romania*

Keywords: Hyperbolic partial differential equation, Contact problem, Method of Lines, Galerkin method, Cellular Neural Networks, Computational methods, Neuromathematics.

Abstract: In this paper we consider a vibrational percussion system described by a one-dimensional hyperbolic partial differential equation with boundary dissipation at one extremity and a normal compliance contact condition at the other extremity. Firstly, we obtain the mathematical model using the *Calculus of variations* and we prove the existence of weak solutions. Secondly, we focus on the numerical approximation of solutions by using a neuromathematics approach – a well-structured numerical technique which combines a specific approach of Method of Lines with the paradigm of Cellular Neural Networks. Our technique ensures from the beginning the requirements for convergence and stability preservation of the initial problem and, exploiting the local connectivity of the approximating system, leads to a low computational effort. A comprehensive set of numerical simulations, considering both contact and non-contact cases, ends the contribution.

1 INTRODUCTION

The purpose of the paper is twofold. Firstly, we verify, on a new mathematical model from *Contact Mechanics*, a well-structured technique for solving hyperbolic partial differential equations (hPDEs), by using *Method of Lines* (MoL) combined with the features and flexibility of *Cellular Neural Networks* (CNNs) – nonlinear processing devices having a large amount of applications from image processing to numerical solving of differential equations. This is a neuromathematics approach, i.e., according to (Galushkin, 2010), an approach used for solving both non-formalized (or weakly formalized) and formalized problems using the neural networks paradigm.

Our approach addresses the formalized-type problems where the structure of the neural network is based only on the "natural parallelism" of the problem itself and does not need a learning process based on experimental data. We have already successfully applied our technique for the overhead crane with non-homogeneous cable (Danciu, 2013a), the torsional stick slip oscillations in oilwell drillstrings (Danciu, 2013b) and the controlled flexible arm of an ocean vessel riser (Danciu and Răsvan, 2014).

It is assumed that our method is even more effective for high dimensions, where the well-organized technique may have the following advantages: a) accuracy (for example, fewer rounding errors), b) robustness to ill numerical conditioning and c) use of existing high-performance software for solving ordinary differential equations (ODEs).

Secondly, we study a particular robotic system of type vibrational percussion system, which is modelled by a one-dimensional hPDE with a dissipative boundary condition at one extremity and a contact nonlinear phenomenon at the other extremity. The study concerns mathematical modelling of the system, existence of the weak solutions for the hPDE problem, numerical approximation and asymptotic behavior. The problem can be viewed as a structure with nonlinear feedback and reference signal. From the mathematical point of view, the main difficulties reside in the nonlinearity of the problem, the lack of a regularization effect of solutions, possibly the effects of discretization on the dissipative mechanism.

The rest of paper is organized as follows. Section 2 deals with mathematical modelling of the system via Calculus of variation methods. Section 3 focuses on the study of the existence of weak solutions for the hPDE problem, whereas Section 4 is devoted to numerical approximation of the solution. We im-

Danciu D., Matei A., Micu S. and Roventa I..
Nonlinear Feedback Control and Artificial Intelligence Computational Methods applied to a Dissipative Dynamic Contact Problem.
DOI: 10.5220/0005055005280539
In *Proceedings of the 11th International Conference on Informatics in Control, Automation and Robotics* (ICINCO-2014), pages 528-539
ISBN: 978-989-758-039-0

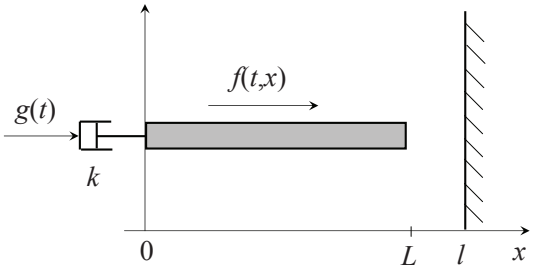

Figure 1: Elastic rod with boundary conditions: 1) a dashpot and time-varying external force at $x = 0$ and 2) a deformable obstacle with normal compliance and initial gap at $x = L$.

plement the approximating system of ODEs by using the CNN paradigm in order to exploit the regularity, parallelism and matrix sparsity of the new problem. The section provides a comprehensive set of numerical simulations, considering both contact and non-contact cases. Concluding remarks end the paper.

2 THE MATHEMATICAL MODEL

We consider an elastic rod with a dashpot attached to the left end $x = 0$. At the opposite extremity $x = L$ the rod can come in contact with a deformable obstacle with normal compliance of stiffness $\frac{1}{\varepsilon}$, $\varepsilon > 0$. The obstacle is located at a distance l (often called the initial gap) to the right of the point $x = L$. The rod is subjected to a body force of density f in the x-direction and to an external force $g(t)$ which acts at the extremity $x = 0$ as shown in Figure 1

In order to obtain the mathematical model, we use the *Calculus of variation* methods. For our case, the kinetic E_k and the potential E_p energies are

$$\begin{aligned} E_k(t) &= \frac{1}{2}\int_0^L \rho(x)A(x)\dot{u}^2(t,x)\mathrm{d}x \\ E_p(t) &= \frac{1}{2}\int_0^L A(x)\sigma^2(t,x)\mathrm{d}x. \end{aligned} \tag{1}$$

Herein, u represents the longitudinal displacement; the internal longitudinal force in the rod is given by $\sigma(x) = Eu_x(t,x)$ where $E > 0$ represents the Young modulus of the material; ρ is the density of the material; A is the cross-sectional area of the rod. In (1) and in the sequel $\dot{u}$ denotes the first time derivative of u and u_x denotes the first derivative with respect to space variable x. Taking into consideration the dissipative forces due to viscous friction at both extremities of the rod $h_0(t)$, $h_1(t)$, the external force $g(t)$ and the axial force of density along the rod $f(t,x)$, the work W_m done by these forces is

$$\begin{aligned} W_m(t) = h_0(t)u(t,0) + g(t)u(t,0) + h_1(t)(u(t,L) - l) \\ + \int_0^1 f(t,x)u(t,x)\mathrm{d}x. \end{aligned} \tag{2}$$

Consider the functional associated to the Hamilton variational principle

$$I(t_1,t_2) = \int_{t_1}^{t_2}(E_k(t) - E_p(t) + W_m(t))\mathrm{d}t \tag{3}$$

with arbitrary t_1, t_2 and introduce the standard Euler-Lagrange variations

$$u(t,x) = \bar{u}(t,x) + \varsigma\mu(t,x) \tag{4}$$

where $\bar{u}(t,x)$ is the basic trajectory and $\varsigma\mu(t,x)$ is the variation of $\bar{u}(t,x)$. The condition for the functional (3) to be minimal along the trajectories of the system will give, after some lengthy but straightforward manipulations, the following equations

$$\begin{aligned} &-\rho(x)A(x)\ddot{\bar{u}} + (A(x)E\bar{u}_x)_x + f(t,x) = 0 \\ &A(0)E\bar{u}_x(t,0) + h_0(t) + g(t) = 0 \\ &-A(L)E\bar{u}_x(t,L) + h_1(t) = 0 \end{aligned} \tag{5}$$

At $x = L$ we shall introduce the contact condition, i.e. the last equation in (5) will be replaced by

$$Eu_x(t,L) = -p(u(t,L) - l), \quad t \in (0,T), \tag{6}$$

with function $p(\cdot)$, having the measure unit of stress, described below in this section. Considering the dissipative force due to the damper, at $x = 0$, $h_0(t) = -ku_t(t,0)$ to be in the opposite direction of motion and, the case of a uniform rod, the equations (5) – (6) become (with an abuse of notation $u := \bar{u}$)

$$\begin{aligned} &\rho(x)A(x)\ddot{u}(t,x) - EA(x)u_{xx}(t,x) = f(t,x) \\ &A(x)Eu_x(t,0) - k\dot{u}(t,0) = -g(t) \\ &Eu_x(t,L) = -p(u(t,L) - l) \end{aligned} \tag{7}$$

Considering $A(x) = A > 0$ and $\rho(x) = \rho > 0$, the mechanical model leads us to the following boundary value problem with initial data

$$\begin{cases} \rho\ddot{u}(t,x) - E\,u_{xx}(t,x) = \frac{1}{A}f(t,x) & x \in (0,L), \\ & t \in (0,T) \\ AEu_x(t,0) = k\dot{u}(t,0) - g(t) & t \in (0,T) \\ Eu_x(t,L) = -p(u(t,L) - l) & t \in (0,T) \\ u(0,x) = u^0(x) & x \in (0,L) \\ \dot{u}(0,x) = u^1(x) & x \in (0,L). \end{cases} \tag{8}$$

where the contact condition is modelled with the following normal compliance function:

$$p(r) = \begin{cases} \varepsilon^{-1} r & \text{if } r \geq 0 \\ 0 & \text{if } r < 0. \end{cases} \quad (9)$$

Herein, ε is the stiffness coefficient. By using the *normal compliance contact condition* (6), the *unilateral Signorini's condition*

$$u(t,L) \leq l,\ u_x(t,L) \leq 0,\ u_x(t,L)(u(t,L)-l) = 0$$

is relaxed; formally, Signorini's nonpenetration condition is obtained in the limit $\varepsilon \to 0$. Thus, the contact with a rigid obstacle can be viewed as a limit case of contact with deformable support whose resistance to compression subsequently increases.

The normal compliance condition was proposed in (Martins and Oden, 1987) with $p(r) = c(r_+)^m$ where $c, m > 0$ and $r_+ = max\{0, r\}$. Then it was used in a large number of publications, see e.g. (Andersson, 1991; Andersson, 1995; Han and Sofonea, 2002; Kikuchi and Oden, 1988; Klarbring and Shillor, 1988; Klarbring and Shillor, 1991; Rochdi and Sofonea, 1998).

3 EXISTENCE OF SOLUTIONS

This section is devoted to study the existence of weak solutions of (8) assuming that $f \in L^2((0,T)\times(0,L))$ and $(u^0, u^1) \in V := H^1(0,L) \times L^2(0,L)$. Without loss of generality but simplifying the writing everywhere in this section, we shall set $E = 1$, $k = 1$ and $\rho \equiv 1$. First of all, note that, if u is a classical solution of (8), we obtain that, for every $v \in H^1(0,L)$, the following relation holds for almost any $t \in [0,T]$

$$\langle \ddot{u}(t), v\rangle + \langle u_x(t), v_x\rangle + (\dot{u}(t,0) + g(t))v(0) + p(u(t,L)-l)v(L) = \langle f(t), v\rangle. \quad (10)$$

In (10) and in the sequel, $\langle\ ,\ \rangle$ denotes the inner product in $L^2(0,L)$. By integrating in time (10), we obtain that, for almost any $t \in [0,T]$,

$$\langle \dot{u}(t), v\rangle - \langle u^1, v\rangle + \int_0^t \langle u_x(s), v_x\rangle\, ds + v(0)\int_0^t g(s)\, ds + (u(t,0) - u^0(0))v(0) + v(L)\int_0^t p(u(s,L)-l)ds = \int_0^t \langle f(s), v\rangle\, ds. \quad (11)$$

These relations allow us to give the definition of a weak solution of (8).

DEFINITION 3.1. *A function $u \in C^1([0,T];L^2(0,L)) \cap C([0,T];H^1(0,L))$ is a weak solution of* (8) *if it verifies* (11) *for any $v \in H^1(0,L)$, $u(0) = u^0$ and $\dot{u}(0) = u^1$.*

Note that a solution $u \in C^2([0,T];L^2(0,T)) \cap C^1([0,T];H^1(0,L))$ of (11), also verifies (10) and it is a strong (classical) solution of (8).

The main result of this section is the following.

THEOREM 3.1. *Given $T > 0$, $u^0 \in H^1(0,L)$, $u^1 \in L^2(0,L)$, $f \in L^2((0,T)\times(0,L))$ and $g \in L^2(0,T)$, equation* (8) *has a weak solution (in the sense of Definition 3.1)*

$$u \in C^1([0,T];L^2(0,L)) \cap C([0,T];H^1(0,L)). \quad (12)$$

For the proof of Theorem 3.1 we use the well-known Galerkin method (see, for instance, (Lions, 1969) and (Kim, 1989) where this method is applied in similar cases). In order to do that, let $(w_k)_{k\geq 1} \subset C^\infty(0,L)$ be a basis of the space $L^2(0,L)$. For each $m \geq 1$, we define the space

$$V_m = \text{Span}\{w_1, ..., w_m\}.$$

Let us first prove three technical lemmas.

LEMMA 3.1. *Let $m \geq 1$. For any $(a_j^0)_{1\leq j\leq m} \in \mathbb{R}^m$ and $(a_j^1)_{1\leq j\leq m} \in \mathbb{R}^m$, there exists a unique function $u_m \in C^2([0,T];V_m)$ which verifies* (10) *for any $v \in V_m$ and it is of the form*

$$u_m(t,x) = \sum_{j=1}^m a_{mj}(t) w_j(x), \quad (13)$$

with $(a_{mj})_{1\leq j\leq m} \subset C^2[0,T]$, $a_{mj}(0) = a_j^0$ and $a'_{mj}(0) = a_j^1$.

Proof. Since any function in $C^2([0,T];V_m)$ is of the form (13) the result follows if we prove that there exists a unique sequence $(a_{mj})_{1\leq j\leq m} \subset C^2[0,T]$ with $a_{mj}(0) = a_j^0$ and $a'_{mj}(0) = a_j^1$ such that for each $1 \leq i \leq m$ we have that

$$\sum_{j=1}^m \ddot{a}_{mj}(t)\langle w_j, w_i\rangle + \sum_{j=1}^m a_{mj}(t)\langle w_{j,x}(t), w_{i,x}\rangle + \sum_{j=1}^m \dot{a}_{mj}(t) w_j(0) w_i(0) + g(t) w_i(0) + p\left(\sum_{j=1}^m a_{mj}(t) w_j(L) - l\right) w_i(L) = \langle f(t), w_i\rangle. \quad (14)$$

In order to simplify the writing we introduce the following notations

$$A = (A_{ji})_{1\leq j,i\leq m} = (\langle w_j, w_i\rangle)_{1\leq j,i\leq m} \in \mathbb{R}^{2m},$$

$$A^{-1} = (\alpha_{ij})_{1\leq j,i\leq m}.$$

Note that, due to the linear independence of the functions $(w_j)_{j\geq 1}$ in $L^2(0,L)$, the matrix A is invertible. For $1 \leq j,i \leq m$ we also note

$$\langle w_{j,x}, w_{i,x}\rangle = \beta_{ji} \in \mathbb{R},\ w_j(0) w_i(0) = \gamma_{ji} \in \mathbb{R},$$

Therefore, the system (14) can be rewritten as follows,

$$\begin{cases} \dot{a}_{mj}(t) &= b_{mj}(t) \\ \dot{b}_{mj}(t) &= c_{mj}(t) \end{cases}$$

where

$$\begin{aligned} c_{mj}(t) = &-\sum_{i=1}^{m}\sum_{k=1}^{m} a_{mk}(t)\alpha_{ji}\beta_{ki} \\ &-\sum_{i=1}^{m}\sum_{k=1}^{m} b_{mk}(t)\alpha_{ji}\gamma_{ki} + g(t)\sum_{i=1}^{m}\alpha_{ji}w_i(0) \\ &- p\left(\sum_{k=1}^{m} a_{mk}(t)w_k(L) - l\right)\sum_{i=1}^{m}\alpha_{ji}w_i(L) \\ &+\sum_{i=1}^{m}\alpha_{ji}\langle f(t), w_i\rangle. \quad (15) \end{aligned}$$

Notice that $c = (c_{m1}, c_{m2}, \ldots, c_{mm})^* \in C([0,T];\mathbb{R}^m)$. Here and in the sequel x^* denotes the adjoint of the vector x.

Let $y \in C^2([0,T];\mathbb{R}^{2m})$, $y = (a,b)^*$, $a = (a_{m1}, a_{m2}, \ldots, a_{mm})^* \in C([0,T];\mathbb{R}^m)$, $b = (b_{m1}, b_{m2}, \ldots, b_{mm})^* \in C([0,T];\mathbb{R}^m)$.

The system (14) can be rewritten now as follows.

$$\dot{y}(t) = F(y)(t)$$

where

$$F : C^2([0,T];\mathbb{R}^{2m}) \to C^2([0,T];\mathbb{R}^{2m}) \quad Fy = (b,c)^*.$$

The function F is a Lipschitz continuous one. Indeed, if we take $t \in [0,T]$ we have that

$$\begin{aligned} &\|(Fy^1 - Fy^2)(t)\|_{\mathbb{R}^{2m}} \\ &\quad \le k_1(\|b^1(t) - b^2(t)\|_{\mathbb{R}^m} + \|c^1(t) - c^2(t)\|_{\mathbb{R}^m}) \\ &\le k_2(\|b^1(t) - b^2(t)\|_{\mathbb{R}^m} + \sum_{j=1}^{m} |{c^1}_{mj}(t) - {c^2}_{mj}(t)|). \end{aligned} \quad (16)$$

Since

$$\begin{aligned} |c^1_{mj}(t) - c^2_{mj}(t)| \le &\sum_{i,k=1}^{m} |a^1_{mk}(t) - a^2_{mk}(t)|\alpha_{ji}\beta_{ki} \\ &+ \sum_{i,k=1}^{m} |b^1_{mk}(t) - b^2_{mk}(t)|\alpha_{ji}\gamma_{ki} \\ &+ \left| p\left(\sum_{k=1}^{m} a^1_{mk}(t)w_k(L) - l\right) - p\left(\sum_{k=1}^{m} a^2_{mk}(t)w_k(L) - l\right)\right| \\ &\times \sum_{i=1}^{m}\alpha_{ji}w_i(L), \quad (17) \end{aligned}$$

as p is a Lipschitz continuous function we deduce that

$$\begin{aligned} |{c^1}_{mj}(t) - {c^2}_{mj}(t)| \le k_3(&\|a^1(t) - a^2(t)\|_{\mathbb{R}^m} \\ &+ \|b^1(t) - b^2(t)\|_{\mathbb{R}^m}). \quad (18) \end{aligned}$$

By (16), (17) and (18) we can write

$$\begin{aligned} &\|(Fy^1 - Fy^2)(t)\|_{\mathbb{R}^{2m}} \\ &\quad \le k_4(\|a^1(t) - a^2(t)\|_{\mathbb{R}^m} + \|b^1(t) - b^2(t)\|_{\mathbb{R}^m}) \\ &\quad \le k_5 \max_{t\in[0,T]} \|y^1(t) - y^2(t)\|_{\mathbb{R}^{2m}}. \quad (19) \end{aligned}$$

Therefore,

$$\|Fy^1 - Fy^2\|_{C([0,T];\mathbb{R}^{2m})} \le k_5\|y^1 - y^2\|_{C([0,T];\mathbb{R}^{2m})}.$$

Since (14) is a system of ordinary differential equations with a Lipschitz nonlinear term, it follows that there exists a unique solution $(a_{mj})_{1\le j\le m} \subset C^2[0,T]$ with $a_{mj}(0) = a^0_j$ and $\dot{a}_{mj}(0) = a^1_j$ of (14). □

LEMMA 3.2. *The sequence $(u_m)_{m\ge1}$ given by Lemma 3.1 is uniformly bounded in the space $L^\infty([0,T];H^1(0,L)) \cap H^1([0,T];L^2(0,L))$.*

Proof. Since u_m verifies (10) for any $v \in V_m$ it follows that,

$$\begin{aligned} &\langle \ddot{u}_m(t), \varphi_m(t)\rangle + \langle u_{m,x}(t), \varphi_{m,x}(t)\rangle \\ &\quad + (\dot{u}_m(t,0) + g(t))\varphi_m(t,0) \\ &+ p(u_m(t,L) - l)\varphi_m(t,L) = \langle f(t), \varphi_m(t)\rangle, \quad (20) \end{aligned}$$

for any $\varphi_m \in C^2([0,T];V_m)$. Now, if we take $\varphi_m = \dot{u}_m$ in (20) we deduce that

$$\begin{aligned} &\frac{d}{dt}\left(\frac{1}{2}\int_0^L \dot{u}_m^2(t,x)\,dx + \frac{1}{2}\int_0^L u_{m,x}^2(t,x)\,dx \right. \\ &\qquad \left. + \frac{\varepsilon}{2}(p(u_m(t,L) - l))^2\right) \\ &+ (\dot{u}_m(t,0))^2 + g(t)\dot{u}_m(t,0) = \langle f(t), \dot{u}_m(t)\rangle. \end{aligned}$$

If we define the energy of the solution by

$$\begin{aligned} E_m(t) = &\frac{1}{2}\int_0^L \dot{u}_m^2(t,x)\,dx + \frac{1}{2}\int_0^L u_{m,x}^2(t,x)\,dx \\ &+ \frac{\varepsilon}{2}(p(u_m(t,L) - l))^2, \end{aligned}$$

we obtain from the previous relation that

$$\frac{d}{dt}E_m(t) \le \langle f(t), \dot{u}_m(t)\rangle + \frac{1}{2}g^2(t).$$

Let $t \in [0,T]$. After integration between 0 and t we get

$$\begin{aligned} E_m(t) \le E_m(0) &+ \int_0^t \frac{1}{2}\int_0^L \dot{u}_m^2(s,x)\,dx\,ds \\ &+ \frac{1}{2}\int_0^t g^2(s)\,ds + \frac{1}{2}\int_0^t\int_0^L f^2(s,x)\,dx\,ds \end{aligned}$$

and from this we deduce

$$E_m(t) \le E_m(0) + \frac{1}{2}\int_0^t g^2(s)\,ds$$

$$+\frac{1}{2}\int_0^t\int_0^L f^2(s,x)\,dx\,ds+\int_0^t E_m(s)\,ds.$$

By using a Gronwall inequality we can write

$$\begin{aligned}E_m(t)&\le\left(E_m(0)+\frac{1}{2}\int_0^t g^2(s)\,ds\right.\\&\quad\left.+\frac{1}{2}\int_0^t\int_0^L f^2(s,x)\,dx\,ds\right)e^t\\&\le\left(E_m(0)+\frac{1}{2}\int_0^t g^2(s)\,ds\right.\\&\quad\left.+\frac{1}{2}\int_0^T\int_0^L f^2(s,x)\,dx\,ds\right)e^T.\end{aligned}$$

Therefore, we have that

$$\begin{aligned}\int_0^L \dot{u}_m^2(t,x)\,dx&\le\left(E_m(0)+\frac{1}{2}\int_0^t g^2(s)\,ds\right.\\&\quad\left.+\frac{1}{2}\int_0^T\int_0^L f^2(s,x)\,dx\,ds\right)e^T,\\\int_0^L u_{m,x}^2(t,x)\,dx&\le\left(E_m(0)+\frac{1}{2}\int_0^t g^2(s)\,ds\right.\\&\quad\left.+\frac{1}{2}\int_0^T\int_0^L f^2(s,x)\,dx\,ds\right)e^T.\end{aligned}$$

The required boundedness properties are straightforward consequences of the last two inequalities. □

LEMMA 3.3. *Suppose that*

$$\sum_{j=1}^m a_j^0 w_j\to u^0 \text{ in } H^1(0,L) \text{ as } m\to\infty, \tag{21}$$

$$\sum_{j=1}^m a_{jm}^1 w_j\to u^1 \text{ in } L^2(0,L) \text{ as } m\to\infty. \tag{22}$$

There exists a subsequence $(u_{m_k})_{k\ge1}$ of the sequence $(u_m)_{m\ge1}$ given by Lemma 3.1 and a function $u\in C^1([0,T];L^2(0,L))\cap C([0,T];H^1(0,L))$ such that

$$u_{m_k}\rightharpoonup^* u \text{ in } L^\infty([0,T];H^1(0,L)) \tag{23}$$

$$u_{m_k}\rightharpoonup u \text{ in } H^1([0,T];L^2(0,L)). \tag{24}$$

Proof. The existence of u follows from the boundedness properties from Lemma 3.2. □

Now we have all the ingredients needed to prove the main result of this section.

Proof of Theorem 3.1. Let u be the function obtained in Lemma 3.3. We prove that u verifies (11). From the linearity and continuity of the left hand side of (11) in $v\in H^1(0,L)$, it follows that (11) is equivalent to

$$\begin{aligned}&\langle\dot{u}(t),w_j\rangle-\langle u^1,w_j\rangle+\int_0^t\langle u_x(s),w_{j,x}\rangle\,ds\\&\quad+(u(t,0)-u^0(0))w_j(0)+g(t)w_j(0)\\&\quad+w_j(L)\int_0^t p(u(s,L)-l)ds=\int_0^t\langle f(s),w_j\rangle\,ds,\end{aligned} \tag{25}$$

for each $j\ge1$. Now, the fact that u verifies (25) follows by taking the limit when m tends to infinity in (14), by using the convergence properties (21)-(24) and by integrating in time from 0 to t. □

Finally, we remark that, from (10), the uniqueness of a classical solution $u\in C^2([0,T];L^2(0,T))\cap C^1([0,T];H^1(0,L))$ of (8) can be easily proved. The uniqueness of a weak solution is more difficult to show and it will be addressed in a future work.

4 NUMERICAL APPROXIMATION OF SOLUTIONS

As Bertrand Russell said, "although this may seem a paradox, all exact science is dominated by the idea of approximation". Numerical approximations are even more useful for problems which cannot be analytically solved. In order to numerically solve the mixed initial boundary value problem for hPDE (8), we consider an approach of Method of Lines which employs the paradigm of Cellular Neural Networks.

The Method of Lines is a general concept rather than a specific method and, can be used for solving hyperbolic PDEs. The overall philosophy is to separately cope with the space and time discretization. The first step is to choose an adequate method for discretizing hPDE with respect to the space variables and incorporate the boundary conditions. "The spectrum of this discrete operator is then used as a guide to choose an appropriate method to integrate the equations through time" (Hyman, 1979).

4.1 The Approximating System Via Method of Lines

The main idea of our numerical technique is the following. For the first step of MoL – the discretization of derivatives with respect to the space coordinates by taking into account the boundary conditions – we use an approach which, according to (Halanay and Răsvan, 1981), ensures for the approximating system

the requirements for convergence and stability preservation of the initial problem. Subsequently, we derive the approximated solution by mapping the new problem – an initial value problem – on an optimal structure of CNNs. Thus, the parallelism and regularities of the new problem are better exploited and, choosing an adequate solver from those already existing in dedicated software packages, the computational effort and storage can be considerably reduced.

4.1.1 Preliminaries

Consider the hPDE problem (8). We introduce the new variables $v(t,x) = \dot{u}(t,x)$ and $w(t,x) = u_x(t,x)$ and write the problem in the Friedrichs form

$$\begin{aligned} &\dot{v}(t,x) - c^2 w_x(t,x) = \tfrac{1}{\rho A} f(t,x) \\ &\dot{w}(t,x) - v_x(t,x) = 0 \end{aligned} \tag{26}$$

where $c = \sqrt{E/\rho}$ is the velocity of propagation for the material of the rod. Note that the system's matrix

$$A = \begin{bmatrix} 0 & -c^2 \\ -1 & 0 \end{bmatrix}$$

has the eigenvalues $\pm c$. Considering, without losing of the generality of the problem, $L = 1$, $\varepsilon = 1$, the boundary conditions (BCs) read as

$$\begin{aligned} &AEw(t,0) - kv(t,0) = -g(t) \\ &Ew(t,1) = -p(z(t)) \\ &z(t) = u(t,1) - l \\ &\dot{z} = v(t,1). \end{aligned} \tag{27}$$

where z is a new variable.

If data are smooth enough, the initial conditions (ICs) can be deduced from (8) and have the following form

$$\begin{aligned} &w(0,x) = w(t,x) \mid_{t=0} = u_x(t,x) \mid_{t=0} = u_x^0(x) \\ &v(0,x) = v(t,x) \mid_{t=0} = \dot{u}(t,x) \mid_{t=0} = u^1(x) \\ &z(0) = u(1,0) - l = u^0(1) - l. \end{aligned} \tag{28}$$

The possible stationary solutions for $f(t,x) = 0$, $g(t) = 0$, $p(\cdot) = 0$, obtained from (26)–(27) by considering the time derivatives to be zero, are

$$\bar{v} = 0, \bar{w} = 0, \bar{z} = u^0(1) - l.$$

Next, we introduce the Riemann invariants r_1 and r_2 as

$$\begin{aligned} r_1(t,x) &= v(t,x) - cw(t,x) \\ r_2(t,x) &= v(t,x) + cw(t,x) \end{aligned} \tag{29}$$

with their transform pair

$$\begin{aligned} v(t,x) &= \tfrac{1}{2}[r_1(t,x) + r_2(t,x)] \\ w(x,t) &= \tfrac{1}{2c}[-r_1(t,x) + r_2(t,x)]. \end{aligned} \tag{30}$$

Thus, we obtained a decoupled PDE system in normal form

$$\begin{aligned} &\frac{\partial r_1}{\partial t}(x,t) + c \cdot \frac{\partial r_1}{\partial x}(x,t) = \frac{1}{\rho A} f(t,x) \\ &\frac{\partial r_2}{\partial t}(t,x) - c \cdot \frac{\partial r_2}{\partial x}(x,t) = \frac{1}{\rho A} f(t,x) \end{aligned} \tag{31}$$

with BCs

$$\begin{aligned} r_1(t,0) &= -a \cdot r_2(t,0) + 2bg(t) \\ r_2(t,1) &= r_1(t,1) - 2dp(z(t)) \\ z(t) &= u(t,1) - l \\ \dot{z}(t) &= \frac{1}{2}[r_1(t,1) + r_2(t,1)] \end{aligned} \tag{32}$$

and ICs

$$\begin{aligned} &r_1(0,x) = v(0,x) - cw(0,x) = u^1(x) - cu_x^0(x) \\ &r_2(0,x) = v(0,x) + cw(0,x) = u^1(x) + cu_x^0(x) \\ &z(0) = u^0(1) - l. \end{aligned} \tag{33}$$

The notations in (32) are as follows

$$a = \frac{k - A\sqrt{\rho E}}{k + A\sqrt{\rho E}},\ b = \frac{1}{k + A\sqrt{\rho E}},\ d = \frac{1}{\sqrt{\rho E}}.$$

4.1.2 The Approximating System of ODEs for the Initial hPDE Problem

As already said, MoL provides algebraic approximations for the space derivatives, thus allowing the conversion of the mixed initial boundary value problem for hPDE into an initial value problem for a high-dimensional system of ODEs.

In the sequel we apply the Method of Lines for the one-dimensional hPDE problem in the normal form (31)–(32)–(33). Firstly, let us observe from (31) that r_1 represents the forward wave and r_2 the backward wave. This information is useful in applying the

Courant-Isaacson-Rees rule for discretization with respect to the space variable x in order to ensure a good coupling with the boundary conditions.

Let us discretize the interval $[0,1]$, where x is defined, with equally spaced points and denote N – the number of intervals, $h = 1/N$ – the discretization step and $x_i = ih$. The approximations for the derivatives with respect to the space variable are performed according to the above-mentioned Courant-Isaacson-Rees rule as follows

- the backward Euler scheme – for the forward wave $r_1(t,x)$,
- the forward Euler scheme – for the backward wave $r_2(t,x)$.

Next, we denote the functions that approximate the two waves at the discrete points x_i: $\xi_1^i(t) \approx r_1(ih,t)$ and $\xi_2^i(t) \approx r_2(ih,t)$, $i = \overline{0,N}$. Without taking into account the BCs and having the axial force of density along the rod $f(t,x) = 0$, we formally obtain for (31) the following system of ODEs, written in the normal Cauchy form

$$\begin{aligned} \dot{\xi}_1^i(t) &= s\xi_1^{i-1} - s\xi_1^i \ , \ i = \overline{1,N} \\ \dot{\xi}_2^i(t) &= -s\xi_2^i + s\xi_2^{i+1} \ , \ i = \overline{0,N-1} \end{aligned} \tag{34}$$

with $s = cN$. From (32), the boundary conditions become

$$\begin{aligned} \xi_1^0(t) &= -a \cdot \xi_2^0(t) + 2bg(t) \\ \xi_2^N(t) &= \xi_1^N(t) - 2dp(z(t)) \\ \dot{z}(t) &= \frac{1}{2}[\xi_1^N(t) + \xi_2^N(t)] \end{aligned} \tag{35}$$

Substituting (35) in (34), the system of ODEs which embeds the boundary conditions is

$$\begin{aligned} \dot{\xi}_1^1(t) &= -sa\xi_2^0 - s\xi_1^1 + 2bg(t) \\ \dot{\xi}_1^i(t) &= s\xi_1^{i-1} - s\xi_1^i \ , \ i = \overline{2,N} \\ \dot{\xi}_2^i(t) &= -s\xi_2^i + s\xi_2^{i+1} \ , \ i = \overline{0,N-2} \\ \dot{\xi}_2^{N-1}(t) &= -s\xi_2^{N-1} + s\xi_1^N - 2sdp(z(t)) \\ \dot{z}(t) &= \xi_1^N - dp(z(t)) \end{aligned} \tag{36}$$

with the initial conditions given by (32)–(33)

$$\begin{aligned} \xi_1^i(0) &= u^1(x_i) - cu_x^0(x_i) \ , \ i = \overline{1,N-1} \\ \xi_2^i(0) &= u^1(x_i) + cu_x^0(x_i) \ , \ i = \overline{1,N-1} \\ \xi_1^N(0) &= u^1(1) - cu_x^0(1) + 2dp(z(0)) \\ \xi_2^0(0) &= -u^1(0) + cu_x^0(0) + \frac{2b}{a}g(0) \\ z(0) &= u^0(1) - l. \end{aligned} \tag{37}$$

Thus, the initial problem – described by a one dimensional hyperbolic partial differential equation with boundary dissipation at one extremity and a normal compliance condition at the other extremity – is converted into the initial value problem (36)–(37). We emphasize that, if the initial and boundary conditions are "matched" in (37), each solution of system (36) approximates the corresponding wave at the discrete point x_i. This is a necessary condition in order to avoid the propagation of the initial discontinuities.

From the dynamical systems point of view, the approximating system (36) can be represented as in Figure 2, i.e. as a structure with nonlinear feedback and reference signal, more specifically, a feedback connection of the nonlinear block $\mu(t) = -p(\sigma(t))$ with the linear block L whose dynamics is described by

$$\begin{aligned} \dot{y}(t) &= Ay + b_1\mu(t) + b_2 g(t) \\ \sigma(t) &= c^T y \end{aligned} \tag{38}$$

where

$$y^T = [\ \xi_1^1 \ \dots \ \xi_1^N \ \xi_2^{N-1} \ \dots \ \xi_2^0 \ z\ ] \tag{39}$$

and A is the matrix of the linear block, $b_1^T = [-2sd \ -d]$, $b_2^T = [2b\ 0]$, $p(\cdot)$ is the nonlinear function and $g(t)$ is a time-varying reference signal.

The linear block L of the nonlinear system has a simple zero eigenvalue and all the rest of the eigenvalues belong to the left half-plane of $\mathbb{C}$. The qualitative analysis of the nonlinear system can be performed via the approach and methods of absolute stability theory – for instance, by using the Popov frequency domain inequalities for the critical case with a simple zero root.

4.2 The CNN Paradigm for Numerical Solution of the Approximating System

Due to the fact that the approximating system of ODEs displays the usual regularities induced by the

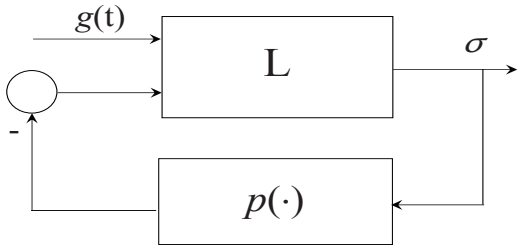

Figure 2: Structure with nonlinear feedback and reference signal.

numerical solving of a PDE problem, one can use the CNN paradigm.

Cellular Neural Networks are artificial recurrent neural networks displaying local interconnections among their cells (identical elementary nonlinear dynamical systems), feature which makes them desirable for processing huge amounts of data even in VLSI implementation. The key idea of the CNNs paradigm resides in representing the interactions among the cells by cloning templates – which can be either translation-invariant or regularly varying templates (Chua and Roska, 1993). Let us briefly introduce their basic characteristics. A general form for the dynamics of a cell in a 2D-array can be described by (Szolgay et al., 1993), (Gilli et al., 2002)

$$\dot{x}_{ij}(t) = \sum_{k,l\in N_r(ij)} T^A_{ij,kl} f(x_{kl}) + \sum_{k,l\in N_r(ij)} T^B_{ij,kl} u_{kl} - \sum_{k,l\in N_r(ij)} T^C_{ij,kl} x_{ij} + I_{ij} \tag{40}$$

where x_{ij} is the state variable of ij^{th} cell, u_{kl} is the input variable from the neighboring cells acting on ij^{th} cell, $N_r(ij)$ – the r-neighborhood of ij^{th} cell, $T^A_{ij,kl}$ is the output feedback cloning template, $T^B_{ij,kl}$ the control cloning template, $T^C_{ij,kl}$ is the state feedback cloning template, I_{ij} is a bias or a constant or time-dependent external stimulus. Usually, the nonlinearity $f(\cdot)$ is the unit bipolar ramp function

$$f(x_{ij}) = \frac{1}{2}(|x_{ij}+1| - |x_{ij}-1|) \tag{41}$$

a bounded, nondecreasing and globally Lipschitzian function, with the Lipschitz constant $L_i = 1$. In some cases, one can consider only the linear part, i.e. $f(x_{ij}) = x_{ij}$.

The problem of representing PDEs via CNNs led to more complex forms for cell dynamics, and it was shown that the flexibility of CNNs allows using them for different approaches in modelling and solving problems having some inherent parallelism and regularities, as it is also the case for PDEs manipulations (op. cit.).

The first step for revealing the one-to-one correspondence between the system of ODEs (36) and a CNN structure is to reorder the equations in (36) for identifying the so-called "cloning templates". For our problem, we can consider the one-dimensional CNN with state vector

$$y^T = [\ \xi_1^1\ \ \xi_1^2\ \ \dots\ \ \xi_1^N\ \ \xi_2^{N-1}\ \ \dots\ \ \xi_2^1\ \ \xi_2^0\ ] \tag{42}$$

and another simple network with the dynamics

$$\dot{z}(t) = y_N + p(z(t)). \tag{43}$$

This arrangement leads to the following simple cloning feedback templates for the inner cells $C_2 \dots C_{2N-1}$:

$$T_i^A = [s\ \ 0\ \ 0]\ ,\ T_i^C = [0\ \ s\ \ 0]\ ,\ i = \overline{2,2N-1}. \tag{44}$$

If, for further computational and simulation tasks, one considers in (40) $f(x_{ij}) = x_{ij}$, one can introduce a template in a compact form which embeds the output feedback template T^A and the decay term template T^C and reads as

$$T_i^{AC} = [s\ \ -s\ \ 0]\ ,\ i = \overline{2,2N-1}. \tag{45}$$

The dynamics of the inner cells of CNN is given by the following equations

$$\begin{aligned} &\dot{y}_i(t) = \begin{bmatrix} s & -s & 0 \end{bmatrix} \begin{bmatrix} y_{i-1} \\ y_i \\ y_{i+1} \end{bmatrix}, \\ &i = \overline{2,N} \cup \overline{N+2,2N-1} \\ &\dot{y}_{N+1}(t) = T^{AC}_{N+1} \cdot y_{N,N+2} + I_{N+1}(t) \end{aligned} \tag{46}$$

with $I_{N+1}(t) = -2sdp(z(t))$.
In the same manner, the dynamics for the corner cells C_1 and C_{2N} is described by

$$\begin{aligned} \dot{y}_1(t) &= -T_1^C y_1 + T_1^A y_{2N} + I_1(t) \\ \dot{y}_{2N}(t) &= -T_{2N}^C y_{2N} + T_{2N}^A y_{2N-1} \end{aligned} \tag{47}$$

with $T_1^C = T_{2N}^C = T_{2N}^A = s$, $T_1^A = -sa$, $I_1 = 2bg(t)$.

If, on the other hand, we consider the closed loop structure induced by (39), the template (45) is also valid for $i = 2N$ which is more convenient from the computational point of view, since there will remain only 3 entries to be separately specified within the matrix T^{AC}.

Another approach will be to consider the vector state

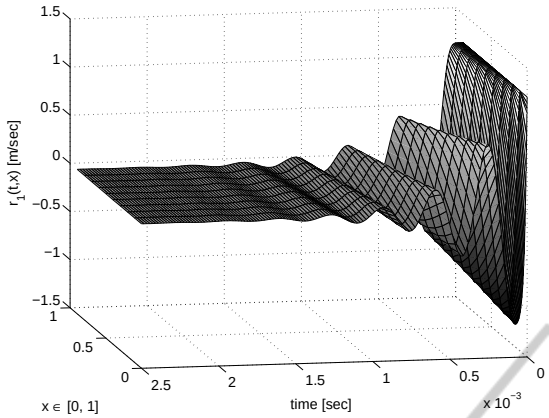

Figure 3: 3D representation of the forward wave $r1(t,x)$ for $g(t)=0$, $f(t,x)=0$ and ICs (50).

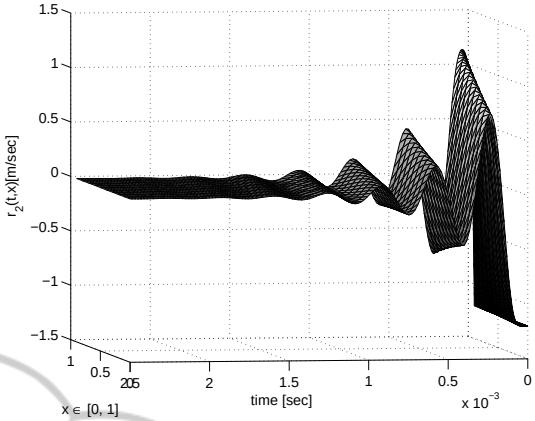

Figure 4: 3D representation of the backward wave $r2(t,x)$ for $g(t)=0$, $f(t,x)=0$ and ICs (50).

$$y^T = [\ \xi_1^1\ \ \xi_1^2\ \ \dots\ \ \xi_1^N\ \ z\ \ \xi_2^{N-1}\ \ \dots\ \ \xi_2^1\ \ \xi_2^0\ ]. \quad (48)$$

This arrangement will give different output feedback cloning template T_i^{AC} and the dynamics for the cells with nonlinear entries will be described by

$$\dot{y}_{N+1}(t) = \begin{bmatrix} 1 & -d & 0 \end{bmatrix} \begin{bmatrix} y_N \\ p(y_{N+1}) \\ y_{N+2} \end{bmatrix}$$

$$\dot{y}_{N+2}(t) = \begin{bmatrix} s & -2sd & -s & 0 & 0 \end{bmatrix} \begin{bmatrix} y_N \\ p(y_{N+1}) \\ y_{N+2} \\ y_{N+3} \\ y_{N+4} \end{bmatrix} \quad (49)$$

with $T_{N+1}^B = T_{N+2}^B = 0$, $I_{N+1} = I_{N+2} = 0$.

Let us observe that for the first proposed arrangement, described by the state vector (42), the matrix for the linear block – the CNN matrix – has the form of a circulant matrix.

5 SIMULATION RESULTS

The results of the simulations allow us to verify the efficiency of the numerical technique, to validate the theoretical results and to understand the physical phenomenon of the propagation of longitudinal vibrations along an elastic rod with boundary constraints and initial conditions described in (8) and Figure 1.

The simulations were performed for the approximating system of ODEs (36). The initial value problem was numerically solved in MATLAB making use of the CNN structure induced by the state vector (39). In this manner the interconnection matrix T_{AC} was found to be an almost bi-diagonal lower matrix (excepting 2 elements ($a_{1,2N}$ and $a_{2N+1,N}$)) with only 3 entries which do not obey the template $T_i^{AC} = [\ s\ \ -s\ 0]$. We have taken advantage of this sparsity property in order to reduce the computational effort and storage.

For the simulation purpose, we considered the following values for the parameters: $E = 288 \cdot 10^6\ \mathrm{N/m^2}$, $\rho = 8\ \mathrm{kg/m^3}$, $L = 1\ \mathrm{m}$, $A = 0.25 \cdot 10^{-4}\ \mathrm{m^2}$, $l = 1.02\ \mathrm{m}$. For the initial conditions, we have taken into account the situation suggested in (Timoshenko, 1937): the rod "compressed by forces applied at the ends, is suddenly released of this compression at $t = 0$". This led in our case to the following ICs:

$$\begin{cases} u^0(x) = 1 + \frac{e}{2} - ex, & x \in [0,1], \quad u^1(x) = 0 \\ 0, & \text{otherwise} \end{cases} \quad (50)$$

with the unit compression $e = 2 \cdot 10^{-4}$. For simulations, the space discretization step $h = 1/10$ was sufficiently small for the convergence of the algorithm (simulations performed with h=1/200 lead to same results).

We have selected 8 figures to show the results of simulations: Figure 3 – Figure 10. Figures 3, 4, 5 present a space-time evolution of the forward and backward waves, as well as the velocity $v(t,x)$ for the following case: the external forces are zero, i.e. $g(t) = 0$, $f(t,x) = 0$ and the damping factor $k = 2 \cdot 10^{-4}$ (very small and of the same order as the time constant of the system). Taking $t \leq 2.5 \cdot 10^{-3}$sec, we focus here on the effects of initial data (50) on the solutions' evolution.

Figures 6, 7, 8, 9, 10 focus on the time evolution of the displacement $u(t,x)$ at the end $x = 1$ of the rod. First two plots show the time evolution of $u(t,1)$ for $g(t) = 0$ and $k = 2 \cdot 10^{-4}$. One can see that the trajectory starts at $u = -10^{-4} = u^0(1) = \xi_1^N(0)$ and the ef-

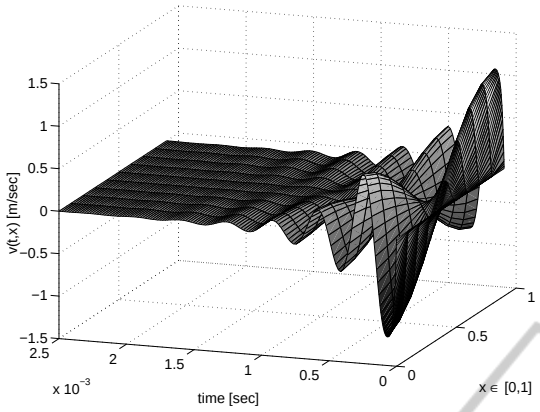

Figure 5: 3D representation of the velocity $v(t,x)$ for $g(t) = 0$, $f(t,x) = 0$ and ICs (50).

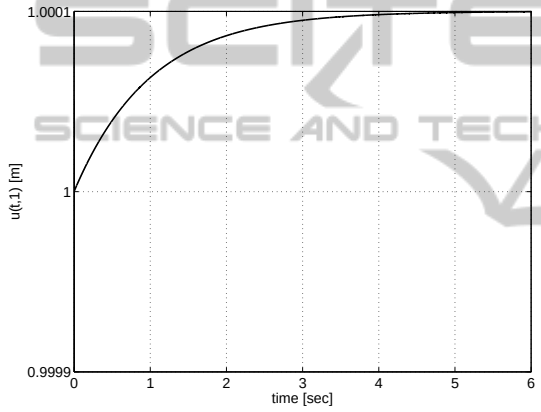

Figure 6: The approximation of the displacement $u(t,x)$ at $x = 1$ for $g(t) = 0$, $k = 2 \cdot 10^{-4}$.

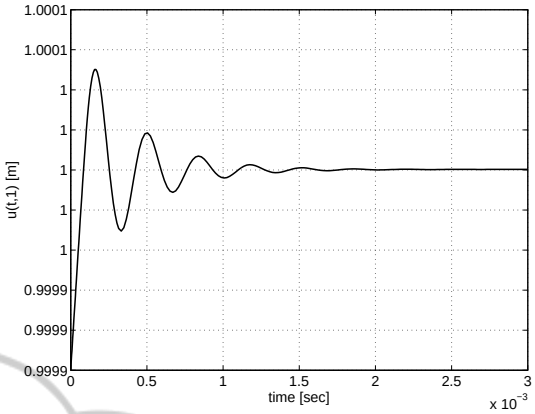

Figure 7: Zoom-in of $u(1,t)$ for $g(t) = 0$ and $k = 2 \cdot 10^{-4}$.

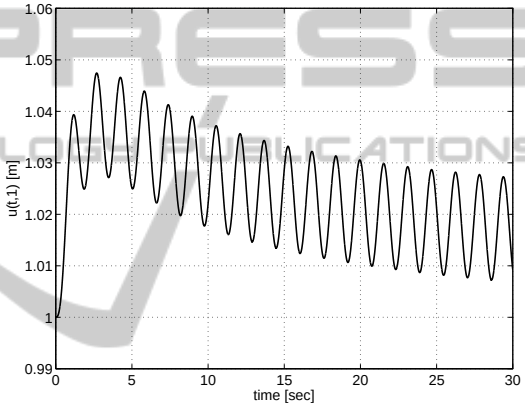

Figure 8: The approximation of the displacement $u(t,x)$ at $x = 1$ for $g(t) = 2sin4t$, $k = 2 \cdot 10^{-4}$.

fects of the initial conditions vanish after 7 time constants (the settling time being $t_s = 1.11 \cdot 10^{-3}$sec). For this case, the rod does not interact with the obstacle, the displacement being smaller than the initial gap.

The last three figures show the time evolution of $u(t,1)$ for a time-varying external stimulus $g(t)$ with $f(t,x) = 0$ and different values of the damping coefficient. Figures 8 and 9 correspond to the case $z > 0$, i.e. the rod interacts with the obstacle at $x = 1$. They reveal the cumulated effects of the initial data, stimulus, the nonlinearity $p(\cdot)$ and of the small damping coefficient related to the amplitude of the stimulus. These factors lead to additional oscillating modes and delay the stabilization.

If, on the other hand, the amplitude of the stimulus is not large enough compared to the damping factor, $z < 0$ and the rod does not penetrate the obstacle, which means $p(z) = 0$. As a consequence, the settling time is short and the movement of the rod is of the same type as the reference signal, $g(t)$, as it is shown in Figure 10.

6 CONCLUSIONS

In this paper we have considered a *Mechanical contact* problem of an elastic rod with a dashpot attached to the left end $x = 0$ and a deformable obstacle with normal compliance at the opposite extremity $x = L$. The rod was subjected to a body force of density f in the x-direction and to an external force $g(t)$ which acts at the extremity $x = 0$. The problem leads to an one-dimensional hyperbolic equation with boundary dissipation at one extremity and a regularized contact law at the other extremity. We proved the existence of weak solutions in the corresponding finite energy space $H^1(0,L) \times L^2(0,L)$. In order to approximate the solution of the problem we used a numerical technique based on an approach of Method of Lines

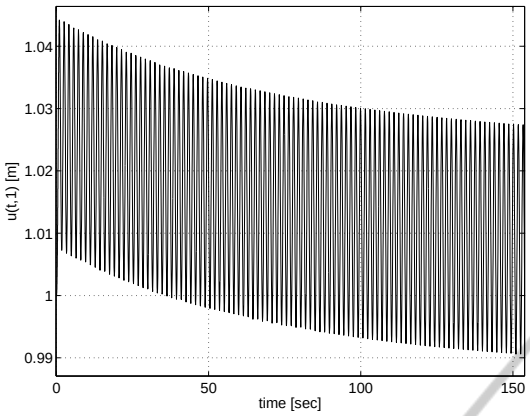

Figure 9: $u(t,x)$ at $x = 1$ for $N = 10$, $g(t) = 5sin4t$, $k = 8 \cdot 10^{-4}$.

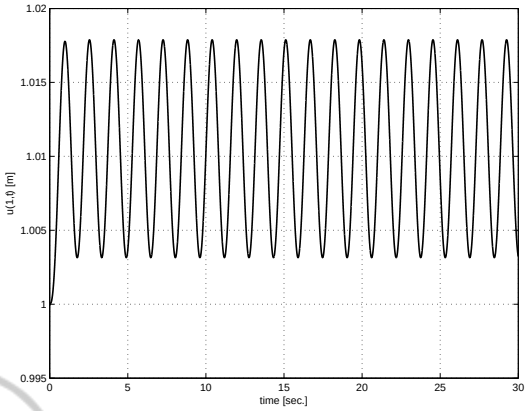

Figure 10: $u(t,x)$ at $x = 1$ for $N = 10$, $g(t) = 2sin4t$, $k = 8 \cdot 10^{-4}$.

which ensures from the beginning the convergence of the approximation and the preservation of stability of the initial problem. Taken into consideration that the conversion of the mixed initial boundary value problem for hPDE into an initial value problem leads to a system of ODEs with a large number of equations and sparse matrix, the numerical implementation and simulations employed the CNN paradigm in order to reduce the computational effort. Considering initial data of the type encountered in engineering applications, the results of simulations allowed the visualization of some hidden behaviors for small scales of time, as well as for long-time behavior.

ACKNOWLEDGEMENTS

This work was partially supported by the grant number 10C/2014, awarded in the internal grant competition of the University of Craiova.

REFERENCES

Andersson, L.-E. (1991). A quasistatic frictional problem with normal compliance. *Nonlinear Analysis TMA*, (16):347–370.

Andersson, L.-E. (1995). A global existence result for a quasistatic contact problem with friction. *Advanced in Mathematical Sciences and Applications*, (5):249–286.

Chua, L. and Roska, T. (1993). The cnn paradigm. *IEEE Trans. Circuits Syst. I*, 40(3):147–156.

Danciu, D. (2013a). *A CNN Based Approach for Solving a Hyperbolic PDE Arising from a System of Conservation Laws - The Case of the Overhead Crane*, Advances in Computational Intelligence, volume 7903, pages 365–374. Springer.

Danciu, D. (2013b). Numerics for hyperbolic partial differential equations (pde) via cellular neural networks (cnn). In *2nd IEEE Int. Conf. on Systems and Computer Science ICSCS'2013*, pages 183–188, Villeneuve d'Ascq, France.

Danciu, D. and Răsvan, V. (2014). *Delays and Propagation: Control Liapunov Functionals and Computational Issues*, chapter 10. Advances in Delays and Dynamics. Springer.

Galushkin, A. I. (2010). *Neural Network Theory*. Springer.

Gilli, M., Roska, T., Chua, L. O., and Civalleri, P. P. (2002). Cnn dynamics represents a broader class than pdes. *I. J. Bifurcation and Chaos*, (10):2051–2068.

Halanay, A. and Răsvan, V. (1981). Approximations of delays by ordinary differential equations. *Recent advances in differential equations*, pages 155–197.

Han, W. and Sofonea, M. (2002). *Quasistatic Contact Problems in Viscoelasticity and Viscoplasticity*. Studies in Advanced Mathematics **30**, American Mathematical Society, Providence, RI—International Press, Somerville, MA.

Hyman, J. (1979). *A method of lines approach to the numerical solution of conservation laws*. Advances in Delays and Dynamics. IMACS Publ. House.

Kikuchi, N. and Oden, J. (1988). *Contact Problems in Elasticity: A Study of Variational Inequalities and Finite Element Methods*. SIAM, Philadelphia.

Kim, J. U. (1989). A boundary thin obstacle problem for a wave equation. *Commun. P. D. E.*, (14):1011–1026.

Klarbring, A. Mikelic, A. and Shillor, M. (1988). Frictional contact problems with normal compliance. *Int. J. Engng. Sci.*, (26):811–832.

Klarbring, A. Mikelic, A. and Shillor, M. (1991). *A global existence result for the quasistatic frictional contact problem with normal compliance*. G. del Piero and F. Maceri, eds., Unilateral Problems in Structural Analysis Vol. 4, Birkhäuser.

Lions, J.-L. (1969). *Quelques methodes de resolution des problmes aux limites non lineaires*. Dunod et Gauthier-Villars, Paris.

Martins, J. A. and Oden, J. T. (1987). Existence and uniqueness results for dynamic contact problems with nonlinear normal and friction interface laws. *Nonlinear Analysis TMA*, (11):407–428.

Rochdi, M. Shillor, M. and Sofonea, M. (1998). Quasistatic viscoelastic contact with normal compliance and friction. *Journal of Elasticity*, (51):105–126.

Szolgay, P., Voros, G., and Eross, G. (1993). On the applications of the cellular neural network paradigm in mechanical vibrating systems. *IEEE Trans. Circuits Syst. I*, 40(3):222–227.

Timoshenko, S. (1937). *Vibration problems in engineering*. D.Van Nostrand Company.